Journal of Organometallic Chemistry 695 (2010) 1493–1498

Contents lists available at ScienceDirect

Journal of Organometallic Chemistry

journal homepage: www.elsevier.com/locate/jorganchem

Systematic study on electrochemical properties of a series of TCNQ lanthanide complexes

Ju-Wen Zhang, Peng-Fei Yan, Guang-Ming Li *, Bin-Qiu Liu, Peng Chen

Key Laboratory of Functional Inorganic Material Chemistry, Heilongjiang University, Ministry of Education, PR China
School of Chemistry and Materials Science, Heilongjiang University, No. 74, Xuefu Road, Nangang District, Harbin 150080, PR China

ARTICLE INFO

Article history:
Received 24 November 2009
Received in revised form 26 February 2010
Accepted 2 March 2010
Available online 6 March 2010

Keywords:
TCNQ
Lanthanide
Synthesis
Structure
Electrochemistry

ABSTRACT

The electrochemical properties of a series of TCNQ (TCNQ = 7,7,8,8-tetracyano-*p*-quinodimethane) lanthanide complexes have been investigated for the first time. Cyclic voltammograms and differential pulse voltammograms of this series of TCNQ lanthanide complexes show a reversible one-electron oxidation and a reversible one-electron reduction within the electrochemical window of CH_3CN. Their electrochemical HOMO–LUMO gap and reversibility are examined. Three new TCNQ lanthanide complexes, namely, $[Ln_2(TCNQ)_4(H_2O)_{12}][2TCNQ]\cdot xMeOH\cdot yH_2O$ [Ln = Ce (**1**, $x = 1$, $y = 3$), Nd (**2**, $x = 2$, $y = 4$), Sm (**3**, $x = 2$, $y = 3$)] have been characterized. X-ray single-crystal diffraction reveals that **1**–**3** are ion complexes with one dimeric cation and two $TCNQ^{\cdot-}$ counterions.

1. Introduction

TCNQ-based metal materials have attracted much attention for several decades due to their conducting and/or magnetic properties [1–7] and their potential applications in erasable photochromic laser disks and memory storage [8–10], organic field-effect transistors [11–13], biosensors [14–16] as well as electrochromic and magnetic devices [17,18]. In particular, the electrical, optical and switching properties of CuTCNQ and AgTCNQ have been widely studied [19–25]. In contrast to CuTCNQ and AgTCNQ, only recently the related binary $M[TCNQ]_2$-based materials (M = Mn, Fe, Co and Ni) have generated a great deal of interest. Dunbar, Miller and their co-workers reported a series of $M[TCNQ]_2$-based materials with significant magnetic properties [26–29]. Bond and co-workers investigated the electrochemical syntheses of these materials [30–32].

However, TCNQ-based lanthanide complexes are rarely known and the research on these complexes has been focused on probing their magnetic properties. Roesky and co-workers reported the first TCNQ-involved lanthanide complex $[\{CuL\}_2Gd(TCNQ)_2]\cdot TCNQ\cdot CH_3OH\cdot 2CH_3CN$ [L = *N*,*N*′-propylenebis(3-methoxysalicylideneiminato)] and its magnetic properties [33]. Dunbar and co-workers reported the second TCNQ lanthanide complex $\{[Gd_2(TCNQ)_5(H_2O)_9][Gd(TCNQ)_4(H_2O)_3]\}\cdot 4H_2O$ and its magnetic properties [34]. Recently, we reported several TCNQ lanthanide complexes $[Ln_2(TCNQ)_4(H_2O)_{10}(EtOH)_2][2TCNQ]\cdot xH_2O$ [Ln = La (**I**, $x = 5$), Pr (**II**, $x = 3$)], $[Ln_2(TCNQ)_4(H_2O)_{10}][2TCNQ]\cdot yH_2O$ [Ln = Gd (**III**, $y = 6$), Dy (**IV**, $y = 5$)] and $[Ln(TCNQ)_2(H_2O)_6][TCNQ]\cdot H_2O\cdot MeOH$ [Ln = Er (**V**), Lu (**VI**)] and investigated their magnetic properties [35]. In contrast with the magnetic properties of TCNQ-based lanthanide complexes, their electrochemical properties are hardly known. In view of the importance of electrochemical syntheses for a series of TCNQ-based transition metal materials [30–32,36,37], we carry out the systematic investigation of electrochemical properties on the series of TCNQ-based lanthanide complexes **1**–**3** and **I**–**VI**.

2. Experimental

2.1. Materials and physical measurements

All reagents and solvents except $LnCl_3\cdot nH_2O$ and Li(TCNQ) were commercially available and used without further purification. $LnCl_3\cdot nH_2O$ were obtained by reacting Ln_2O_3 with hydrochloric acid in aqueous solvent. Li(TCNQ) was prepared according to the literature method [38]. Elemental analyses were carried out on a Perkin–Elmer 2400 analyzer. The FT-IR data were collected on a Perkin–Elmer 60000 spectrophotometer using KBr disks in the range of 4000–370 cm^{-1}. The UV spectra were recorded on a Shimadzu UV2240 spectrophotometer.

2.2. Electrochemistry

Cyclic voltammetry (CV) and differential pulse voltammetry (DPV) measurements were performed on a CHI650C electrochem-

* Corresponding author at: School of Chemistry and Materials Science, Heilongjiang University, No. 74, Xuefu Road, Nangang District, Harbin 150080, PR China. Tel.: +86 451 86608428; fax: +86 451 86604799.
E-mail address: gmli_2000@163.com (G.-M. Li).

0022-328X/$ - see front matter © 2010 Elsevier B.V. All rights reserved.
doi:10.1016/j.jorganchem.2010.03.002

Table 1
Crystal data and structural refinement for **1**–**3**.

	1	2	3
Formula	$C_{73}H_{58}N_{24}O_{16}Ce_2$	$C_{74}H_{64}N_{24}O_{18}Nd_2$	$C_{74}H_{64}N_{24}O_{17}Sm_2$
Formula weight	1807.67	1865.97	1862.19
Shape	Block	Block	Block
Color	Purple	Purple	Purple
Crystal system	Triclinic	Triclinic	Triclinic
Space group	$P\bar{1}$	$P\bar{1}$	$P\bar{1}$
a (Å)	11.937(2)	11.910(2)	11.877(2)
b (Å)	13.387(3)	13.416(3)	13.405(3)
c (Å)	13.878(3)	13.849(3)	13.814(3)
α (°)	106.51(3)	106.32(3)	106.27(3)
β (°)	101.90(3)	101.87(3)	101.99(3)
γ (°)	100.78(3)	100.57(3)	100.45(3)
V (Å^3)	2008.0(9)	2008.5(7)	1996.9(7)
Z	1	1	1
ρ (g cm^{-3})	1.495	1.543	1.548
μ (mm^{-1})	1.199	1.362	1.538
F(0 0 0)	908	940	936
θ range (°)	3.14–27.48	3.06–27.48	3.07–27.48
Reflections collected	18 942	18 504	19 620
Unique reflections	8834	8866	9038
R_{int}	0.0730	0.0882	0.0361
R_1, wR_2 ($I > 2\sigma(I)$) (final)	0.0782, 0.2010	0.0866, 0.2145	0.0409, 0.1006
R_1, wR_2 (all data)	0.1245, 0.2402	0.1258, 0.2575	0.0506, 0.1052
Goodness-of-fit (GOF) on F^2	1.022	1.071	1.049

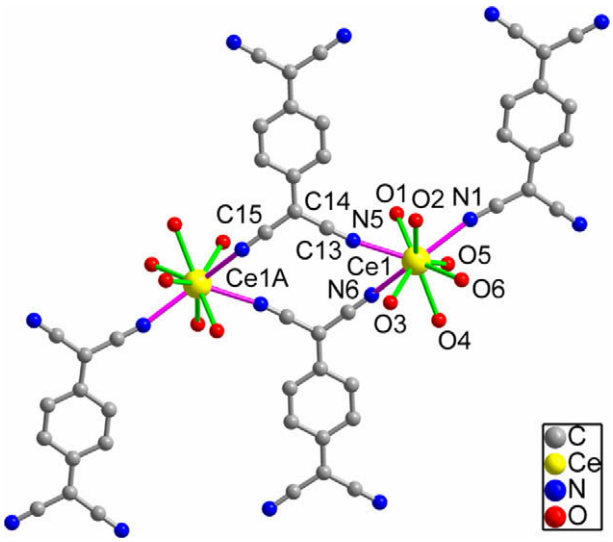

Fig. 1. Cationic structure of **1**. All hydrogen atoms are omitted for clarity.

ical analyzer using a standard three-electrode system (a working electrode/glassy carbon, an auxiliary electrode/platinum mesh and a reference electrode/Ag/AgCl) at room temperature. The working electrode was polished with 30–50 nm alumina slurry on the polishing cloth and rinsed copiously with water and ethanol in an ultrasonic bath prior to use. Nitrogen gas was used to sparge the acetonitrile solution of n-Bu_4NPF_6 (0.1 mol L^{-1}) as supporting electrolyte in which the three electrodes were placed. Complexes

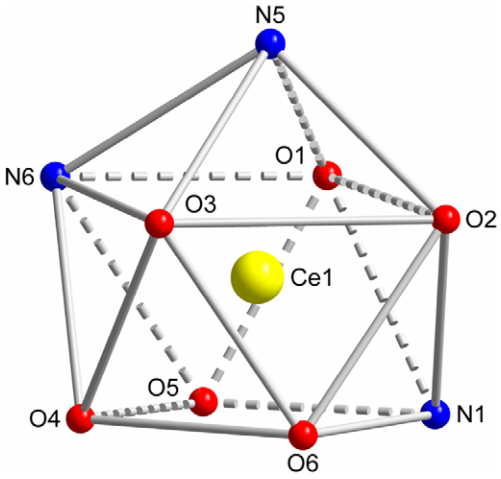

Fig. 2. Perspective view for the coordination geometry of Ce(III) ion in **1**.

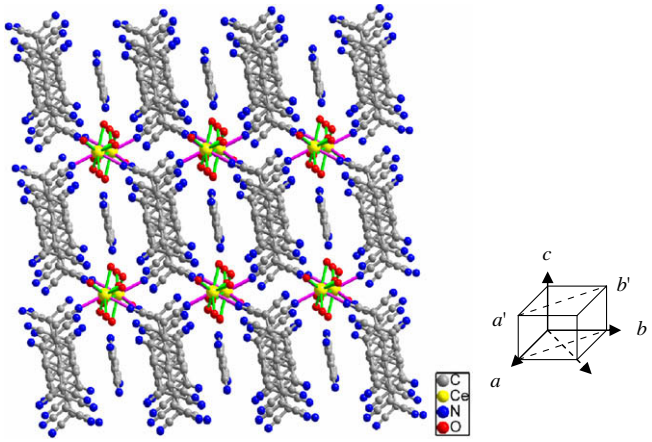

Fig. 3. Packing structure of **1** viewed in the $abb'a'$ plane. All hydrogen atoms and interstitial solvents are omitted for clarity.

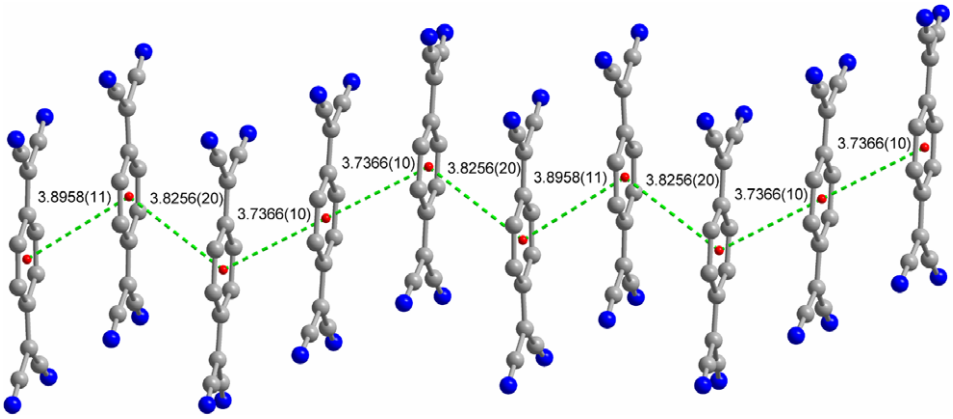

Fig. 4. Side view of the π–π stacking between $TCNQ^{\cdot-}$ radicals in **1**.

1–**3**, **I**–**VI** and TCNQ were modified onto the working electrode by drop-casting method [39]. CV curves were recorded at a scan rate of 100 mV s^{-1} from −0.75 to 0.75 V. DPV curves were recorded at a scan rate of 20 mV s^{-1} with pulse width of 50 ms and sample width of 16.7 ms. The ferrocene/ferrocenium ($Fc^{0/+}$) potential [$E_{1/2}(Fc^{0/+})$] is 0.436 V versus the Ag/AgCl electrode.

2.3. Synthesis of $[Ln_2(TCNQ)_4(H_2O)_{12}][2TCNQ]\cdot xMeOH\cdot yH_2O$ [Ln = Ce (**1**, x = 1, y = 3), Nd (**2**, x = 2, y = 4), Sm (**3**, x = 2, y = 3)]

All reactions and manipulations were carried out by standard Schlenk techniques under nitrogen atmosphere. Purple crystals were synthesized by slow diffusion of $LnCl_3\cdot nH_2O$ (0.1 mmol) in 20 mL degassed MeOH into Li(TCNQ) (0.3 mmol) in 20 mL degassed H_2O in Schlenk tubes.

Complex **1**, yield: 40%. Anal. Calc. for $C_{73}H_{58}N_{24}O_{16}Ce_2$ (1807.67, wt%): C, 48.50; H, 3.23; N, 18.60. Found: C, 48.38; H, 3.41; N, 18.47%. IR (KBr, cm^{-1}): 3202 (m), 2172 (s, ν(C≡N)), 1636 (w), 1572 (s), 1501 (s), 1384 (w), 1319 (s), 1224 (w), 1168 (s), 985 (w), 832 (w), 820 (m), 717 (w), 579 (w), 546 (w), 478 (m). UV (CH_3CN, nm): λ_{max}, 394.

Complex **2**, yield: 50%. Anal. Calc. for $C_{74}H_{64}N_{24}O_{18}Nd_2$ (1865.97, wt%): C, 47.63; H, 3.46; N, 18.02. Found: C, 47.49; H, 3.63; N, 17.84%. IR (KBr, cm^{-1}): 3232 (m), 2177 (s, ν(C≡N)), 1640 (w), 1572 (s), 1500 (s), 1384 (w), 1318 (s), 1224 (w), 1168 (s), 985 (w), 835 (w), 819 (m), 718 (w), 583 (w), 550 (w), 478 (m). UV (CH_3CN, nm): λ_{max}, 394.

Complex **3**, yield: 45%. Anal. Calc. for $C_{74}H_{64}N_{24}O_{17}Sm_2$ (1862.19, wt%): C, 47.73; H, 3.46; N, 18.05. Found: C, 47.61; H, 3.59; N, 18.01%. IR (KBr, cm^{-1}): 3244 (m), 2168 (s, ν(C≡N)), 1648 (w), 1572 (s), 1498 (s), 1384 (w), 1317 (s), 1224 (w), 1168 (s), 985 (w), 836 (w), 818 (m), 713 (w), 583 (w), 546 (w), 477 (m). UV (CH_3CN, nm): λ_{max}, 394.

2.4. Single-crystal structure determination

Crystal data for **1**–**3** were collected on a Rigaku Raxis-Rapid X-ray diffractometer with graphite-monochromated Mo Kα radiation (λ = 0.71073 Å) at 293 K. The structures were solved by direct methods using the program SHELXS-97 and all non-hydrogen atoms were refined anisotropically on F^2 by the full-matrix least-squares technique using the SHELXL-97 crystallographic software package [40,41]. Pertinent crystal data and structural refinement for **1**–**3** are listed in Table 1.

3. Results and discussion

3.1. Synthesis

The TCNQ lanthanide complexes **1**–**3** were synthesized by slowly diffusing a methanol solution of $LnCl_3\cdot nH_2O$ into a water solution of Li(TCNQ). The synthetic method is similar to that of **I**–**VI** and different from that of the reported TCNQ gadolinium complex [34]. The differences of the synthetic methods between **1**–**3** and **I**–**VI** and the TCNQ gadolinium complex in Ref. [34] lead to their distinct structures, which has been discussed in detail in Ref. [35].

3.2. Crystal structure description

X-ray crystallography analysis reveals that **1**–**3** are isostructural ion complexes, so only the structure of **1** is described in detail. **1** crystallizes in the triclinic space group $P\bar{1}$. The molecular structure of **1** consists of one $[Ce_2(TCNQ)_4(H_2O)_{12}]^{2+}$ cation, two $TCNQ^{\cdot-}$ anions, one interstitial MeOH molecule and three interstitial H_2O

Table 2
Important structural parameters for **1**–**3** and **I**–**VI**.

	I[a] (La)	**II**[a] (Pr)	**1** (Ce)	**2** (Nd)	**3** (Sm)	**III**[a] (Gd)	**IV**[a] (Dy)	**V**[a] (Er)	**VI**[a] (Lu)
Ln–N (Å)	2.659(5)–2.690(5)	2.628(5)–2.660(5)	2.636(7)–2.649(7)	2.605(9)–2.621(8)	2.575(4)–2.604(4)	2.514(5)–2.546(5)	2.483(4)–2.521(4)	2.421(4)–2.502(3)	2.282(3)–2.385(3)
Ln–O (Å)	2.501(5)–2.577(4)	2.459(5)–2.552(6)	2.465(6)–2.571(7)	2.450(7)–2.524(8)	2.402(3)–2.509(4)	2.365(5)–2.481(9)	2.313(5)–2.365(5)	2.304(3)–2.352(3)	2.337(3)–2.417(3)
Ln1···Ln1A (Å)	8.634	8.582	8.577	8.553	8.505	8.394	8.329	–	–
Coordination number	9	9	9	9	9	8	8	8	8

[a] Reported by Ref. [35].

molecules. As shown in Fig. 1, the cationic structure of **1** exhibits a dimeric moiety [$Ce_2(TCNQ)_2$]. Two Ce(III) ions are bridged by two $TCNQ^{\cdot-}$ radicals to form a distorted rhombus with a Ce1···Ce1A distance of 8.577 Å. The interior angles 1 (∠N5–Ce1–N6) and 2 (∠C13–C14–C15) are 70.04° and 114.83°, respectively. Each Ce(III) ion is nine-coordinated by three nitrogen atoms from three $TCNQ^{\cdot-}$ radicals and six oxygen atoms from six water molecules. The nine-coordinated atoms around Ce(III) form a distorted monocapped square antiprismatic coordination geometry (Fig. 2). One of two quadrangular faces is defined by one nitrogen atom from one μ_2-$TCNQ^{\cdot-}$ radical and three oxygen atoms from three water molecules (N6, O1, O2 and O3) and the other one is defined by one nitrogen atom from one terminal $TCNQ^{\cdot-}$ radical and three oxygen atoms from other three water molecules (N1, O4, O5 and O6). The dihedral angle between two quadrangular faces is *ca.* 3.33°. The bond lengths of Ce–N are in the range of 2.636(7)–2.649(7) Å and Ce–O in the range of 2.465(6)–2.571(7) Å. Three different modes for $TCNQ^{\cdot-}$ are observed in **1**, namely, μ_2-$TCNQ^{\cdot-}$, terminal $TCNQ^{\cdot-}$ and uncoordinated $TCNQ^{\cdot-}$.

The packing structure of **1** is shown in Fig. 3. The dangling nitrile substituents of the $TCNQ^{\cdot-}$ radicals and the coordinated water molecules form intermolecular hydrogen bonds that connect the dimeric cations to afford a two-dimensional network structure. The π–π stacking interactions between $TCNQ^{\cdot-}$ radicals generate the one-dimensional columns (Fig. 4). There are also $TCNQ^{\cdot-}$ radicals that do not participate in the π–π stacking interactions. They occupy the one-dimensional channels that are perpendicular to the *abb′a′* plane and run throughout the crystal. As a result, the intermolecular hydrogen bonds, π–π stacking interactions and electrostatic interactions coexist in **1** [34,35].

The molecular and packing structures of **1**–**3** are similar to those of **I**–**IV**. The important bond lengths and coordination numbers for **1**–**3** and **I**–**VI** are summarized in Table 2. In all **1**–**3** and **I**–**VI**, the Ln–N (except **1**), Ln–O (except **VI**) and Ln1···Ln1A (except **1**) distances show a continuous decrease along with the size of the lanthanide ions from the largest La(III) ion to the smallest Lu(III) ion. The Ln(III) ions in **1**–**3**, **I** and **II** are nine-coordinated, while the Ln(III) ions in **III**–**VI** are eight-coordinated. The cationic structure of **1**–**3** and **I**–**IV** consists of a dimer, whereas the cationic structure of **V** and **VI** exists in the form of monomer. The change trend of the important structural parameters for **1**–**3** and **I**–**VI** basically accords with the law of lanthanide contraction.

3.3. Electrochemical properties

The solid state electrochemical behavior of **1**–**3**, **I**–**VI** and TCNQ was comparatively investigated by cyclic voltammetry (CV) and differential pulse voltammetry (DPV) in CH_3CN solution of *n*-Bu_4NPF_6 (0.1 mol L^{-1}). The CV and DPV curves of **1** and TCNQ are shown in Fig. 5. The CV and DPV curves of **2**, **3** and **I**–**VI** are similar to those of **1**. The important DPV parameters are summarized in Table 3. According to the CV and DPV curves, all **1**–**3** and **I**–**VI** undergo a reversible one-electron oxidation and a reversible one-electron reduction within the electrochemical window of CH_3CN.

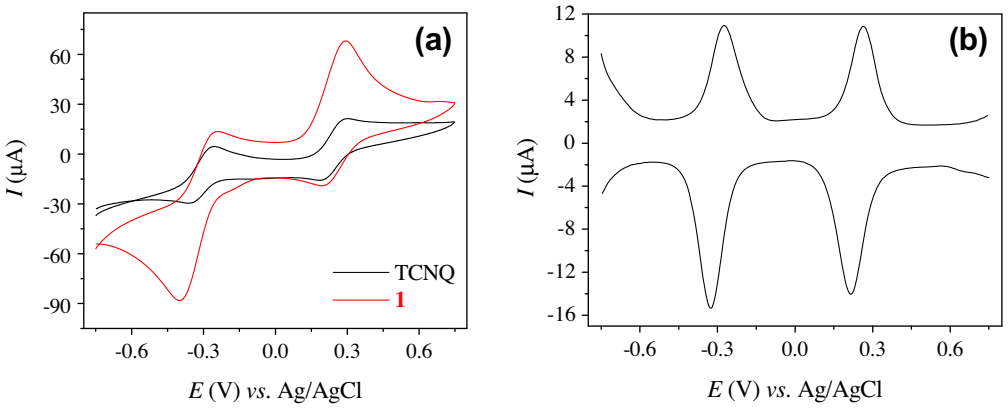

Fig. 5. Cyclic voltammograms of **1** and TCNQ (a) and differential pulse voltammograms of **1** (b).

Table 3
Important DPV parameters of TCNQ, **1**–**3** and **I**–**VI** (*E*, V *vs.* Ag/AgCl; *I*, μA).

	Oxidation							Reduction							$\Delta E^{\circ}_{1/2}$ [a]
	E_{pa}	I_{pa}	E_{pc}	I_{pc}	I_{pc}/I_{pa}	ΔE_p	$E_{1/2}$	E_{pa}	I_{pa}	E_{pc}	I_{pc}	I_{pc}/I_{pa}	ΔE_p	$E_{1/2}$	
TCNQ	0.218	−25.19	0.262	16.48	0.654	0.044	0.240	−0.326	−25.94	−0.286	15.41	0.594	0.040	−0.306	0.546[b]
I (La)	0.214	−20.32	0.278	10.76	0.530	0.064	0.246	−0.318	−17.34	−0.266	4.019	0.232	0.052	−0.292	0.538
II (Pr)	0.214	−17.17	0.266	9.265	0.540	0.052	0.240	−0.318	−10.80	−0.270	4.745	0.439	0.048	−0.294	0.534
1 (Ce)	0.214	−14.05	0.262	10.86	0.773	0.048	0.238	−0.326	−15.33	−0.274	10.93	0.713	0.052	−0.300	0.538
2 (Nd)	0.214	−18.16	0.278	11.62	0.640	0.064	0.246	−0.318	−11.61	−0.282	6.243	0.538	0.036	−0.300	0.546
3 (Sm)	0.214	−14.92	0.282	10.05	0.674	0.068	0.248	−0.310	−10.40	−0.266	5.205	0.500	0.044	−0.288	0.536
III (Gd)	0.218	−17.57	0.266	10.66	0.607	0.048	0.242	−0.322	−13.97	−0.282	5.245	0.375	0.040	−0.302	0.544
IV (Dy)	0.218	−24.03	0.266	18.23	0.759	0.048	0.242	−0.322	−20.74	−0.278	10.76	0.519	0.044	−0.300	0.542
V (Er)	0.218	−14.98	0.270	9.355	0.624	0.052	0.244	−0.318	−10.33	−0.266	4.523	0.438	0.052	−0.292	0.536
VI (Lu)	0.218	−22.53	0.282	14.17	0.629	0.064	0.250	−0.310	−13.65	−0.266	5.804	0.425	0.044	−0.288	0.538

[a] $\Delta E^{\circ}_{1/2}$ is the half-wave redox potential difference between the oxidation and reduction processes, i.e. the electrochemical HOMO–LUMO gap.
[b] Reported by Ref. [31].

$$[TCNQ]^0 \underset{Oxd}{\overset{-e}{\rightleftharpoons}} [TCNQ]^- \underset{Red}{\overset{+e}{\rightleftharpoons}} [TCNQ]^{2-}$$

$$[Ln_x(TCNQ)_y]^+ \underset{Oxd}{\overset{-e}{\rightleftharpoons}} [Ln_x(TCNQ)_y]^0 \underset{Red}{\overset{+e}{\rightleftharpoons}} [Ln_x(TCNQ)_y]^-$$

Scheme 1. One-electron redox processes of TCNQ, **1**–**3** and **I**–**VI**.

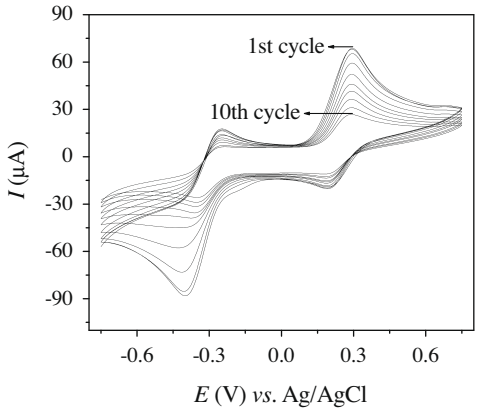

Fig. 6. The 1st–10th cycle for **1**.

Since the oxidation state of the central trivalent lanthanide ions (except cerium ion) does not change, these redox processes are attributed to the removal or addition of electron from or to ligand-based orbitals that are illustrated in Scheme 1, where the oxidation is labeled as Oxd and the reduction as Red.

The half-wave redox potentials of the reduction processes and most of the oxidation processes for **1**–**3** and **I**–**VI** are more positive in contrast to free $TCNQ^{\cdot-}$ (Table 3). It is proposed that the reductions of $TCNQ^{\cdot-}$ in **1**–**3** and **I**–**VI** are easier than that of free $TCNQ^{\cdot-}$, whereas the oxidations become harder. Because $TCNQ^{\cdot-}$ gives electrons in forming the coordinate bonds that facilitates the reduction of $TCNQ^{\cdot-}$. The half-wave redox potential differences between the oxidation and reduction processes for **1**–**3** and **I**–**VI**, $\Delta E^{\circ}_{1/2}$, span a very narrow range of 0.534–0.546 V (Table 3), which indicates that the lanthanide ions have a slight influence on the electrochemical HOMO–LUMO gap (0.546 V) of $TCNQ^{\cdot-}$.

The 1st–10th cycle of **1** show that the current values sharply weaken, while the potential values almost remain invariable (Fig. 6). It may be attributed to the rapid dissolution and/or solubility of **1** and the generated products. The 1st–10th cycles of **2**, **3** and **I**–**VI** are similar to that of **1**. The results of the 1st–10th cycle suggest that the electrochemical properties of **1**–**3** and **I**–**VI** are chemically and electrochemically reversible.

4. Conclusions

The electrochemical study reveals that the lanthanide ions have a slight influence on the electrochemical HOMO–LUMO gap of $TCNQ^{\cdot-}$ and there is no clear relationship between structure and electrochemistry for this series of TCNQ lanthanide complexes. The structures of **1**–**3** are essentially similar to their lanthanum analog. The important structural parameters demonstrate again that the size of the lanthanide ions dominates the structures in this series of TCNQ lanthanide complexes. These results may provide basic information for the electrochemical syntheses of the TCNQ-based lanthanide complexes with different structures and electrochemical properties. Efforts to synthesize electrochemically the TCNQ-based lanthanide materials are currently in progress.

Acknowledgements

This work is financially supported by the National Natural Science Foundation of China (Nos. 20872030, 20972043 and 50903028), Heilongjiang Province (Nos. GC09A402 and 2009RFXXG201) and Heilongjiang University.

Appendix A. Supplementary material

CCDC 625135, 625130 and 625131 contain the supplementary crystallographic data for complexes **1**, **2** and **3**. These data can be obtained free of charge from The Cambridge Crystallographic Data Centre via http://www.ccdc.cam.ac.uk/data_request/cif.

Supplementary data associated with this article can be found, in the online version, at doi:10.1016/j.jorganchem.2010.03.002.

References

[1] O.H. LeBlanc Jr., J. Chem. Phys. 42 (1965) 4307–4308.
[2] W. Kaim, M. Moscherosch, Coord. Chem. Rev. 129 (1994) 157–193.
[3] K. Xiao, I.N. Ivanov, A.A. Puretzky, Z. Liu, D.B. Geohegan, Adv. Mater. 18 (2006) 2184–2188.
[4] K. Xiao, J. Tao, Z. Pan, A.A. Puretzky, I.N. Ivanov, S.J. Pennycook, D.B. Geohegan, Angew. Chem., Int. Ed. 46 (2007) 2650–2654.
[5] H. Miyasaka, T. Izawa, N. Takahashi, M. Yamashita, K.R. Dunbar, J. Am. Chem. Soc. 128 (2006) 11358–11359.
[6] N. Motokawa, T. Oyama, S. Matsunaga, H. Miyasaka, K. Sugimoto, M. Yamashita, N. Lopez, K.R. Dunbar, Dalton Trans. (2008) 4099–4102.
[7] Q.-Y. Lv, S.-D. Tang, X.-W. Tan, W.-J. Lei, Y. Wang, H.-K. Lin, Z.-Q. Wu, S.-Z. Zhan, J. Organomet. Chem. 694 (2009) 3242–3246.
[8] O.K. Cho, K.Y. Park, Mol. Cryst. Liq. Cryst. 267 (1995) 393–398.
[9] S. Yamaguchi, R.S. Potember, Synth. Met. 78 (1996) 117–126.
[10] H. Peng, Z. Chen, L. Tong, X. Yu, C. Ran, Z. Liu, J. Phys. Chem. B 109 (2005) 3526–3530.
[11] A.R. Brown, D.M. de Leeuw, E.J. Lous, E.E. Havinga, Synth. Met. 66 (1994) 257–261.
[12] E. Menard, V. Podzorov, S.H. Hur, A. Gaur, M.E. Gershenson, J.A. Rogers, Adv. Mater. 16 (2004) 2097–2101.
[13] C. Di, G. Yu, Y. Liu, X. Xu, D. Wei, Y. Song, Y. Sun, Y. Wang, D. Zhu, J. Liu, X. Liu, D. Wu, J. Am. Chem. Soc. 128 (2006) 16418–16419.
[14] S. Wakida, Y. Kohigashi, H. Miyamura, K. Higashi, Y. Ujihira, Anal. Sci. 12 (1996) 989–991.
[15] F. Palmisano, P.G. Zambonin, D. Centonze, M. Quinto, Anal. Chem. 74 (2002) 5913–5918.
[16] M. Cano, B. Palenzuela, R. Rodriguez-Amaro, Electroanalysis 18 (2006) 1068–1074.
[17] A. Yasuda, J. Seto, J. Electroanal. Chem. 247 (1988) 193–202.
[18] D.F. Perepichka, M.R. Bryce, C. Pearson, M.C. Petty, E.J.L. McInnes, J.P. Zhao, Angew. Chem., Int. Ed. 42 (2003) 4636–4639.
[19] R.S. Potember, T.O. Poehler, R.C. Benson, Appl. Phys. Lett. 41 (1982) 548–550.
[20] J.J. Hoagland, X.D. Wang, K.W. Hipps, Chem. Mater. 5 (1993) 54–60.
[21] S. Sun, X. Xu, P. Wu, D. Zhu, J. Mater. Sci. Lett. 17 (1998) 719–721.
[22] X.-L. Mo, G.-R. Chen, Q.-J. Cai, Z.-Y. Fan, H.-H. Xu, Y. Yao, J. Yang, H.-H. Gu, Z.-Y. Hua, Thin Solid Films 436 (2003) 259–263.
[23] Y. Liu, Z. Ji, Q. Tang, L. Jiang, H. Li, M. He, W. Hu, D. Zhang, L. Jiang, X. Wang, C. Wang, Y. Liu, D. Zhu, Adv. Mater. 17 (2005) 2953–2957.
[24] R. Müller, J. Genoe, P. Heremans, Appl. Phys. Lett. 88 (2006) 242105-1–242105-3.
[25] C. Zhao, A.M. Bond, J. Am. Chem. Soc. 131 (2009) 4279–4287.
[26] H. Zhao, R.A. Heintz, K.R. Dunbar, R.D. Rogers, J. Am. Chem. Soc. 118 (1996) 12844–12845.
[27] H. Zhao, R.A. Heintz, X. Ouyang, K.R. Dunbar, C.F. Campana, R.D. Rogers, Chem. Mater. 11 (1999) 736–746.
[28] R. Clerac, S. O'Kane, J. Cowen, X. Ouyang, R. Heintz, H. Zhao, M.J. Bazile Jr., K.R. Dunbar, Chem. Mater. 15 (2003) 1840–1850.
[29] E.B. Vickers, I.D. Giles, J.S. Miller, Chem. Mater. 17 (2005) 1667–1672.
[30] A. Nafady, A.P. O'Mullane, A.M. Bond, A.K. Neufeld, Chem. Mater. 18 (2006) 4375–4384.
[31] A. Nafady, A.M. Bond, A. Bilyk, A.R. Harris, A.I. Bhatt, A.P. O'Mullane, R. De Marco, J. Am. Chem. Soc. 129 (2007) 2369–2382.
[32] A. Nafady, A.M. Bond, A. Bilyk, J. Phys. Chem. C 112 (2008) 6700–6709.
[33] A.M. Madalan, H.W. Roesky, M. Andruh, M. Noltemeyer, N. Stanica, Chem. Commun. (2002) 1638–1639.
[34] H. Zhao, M.J. Bazile Jr., J.R. Galán-Mascarós, K.R. Dunbar, Angew. Chem., Int. Ed. 42 (2003) 1015–1018.
[35] J. Zhang, P. Yan, G. Li, G. Hou, M. Suda, Y. Einaga, Dalton Trans. (2009) 10466–10473.
[36] A.K. Neufeld, A.P. O'Mullane, A.M. Bond, J. Am. Chem. Soc. 127 (2005) 13846–13853.

[37] A.R. Harris, A. Nafady, A.P. O'Mullane, A.M. Bond, Chem. Mater. 19 (2007) 5499–5509.
[38] L.R. Melby, R.J. Harder, W.R. Hertler, W. Mahler, R.E. Benson, W.E. Mochel, J. Am. Chem. Soc. 84 (1962) 3374–3387.
[39] C.F. Hogan, A.M. Bond, A.K. Neufeld, N.G. Connelly, E. Liamas-Rey, J. Phys. Chem. A 107 (2003) 1274–1283.
[40] G.M. Sheldrick, SHELXS-97, Program for Solution of Crystal Structures, University of Göttingen, Germany, 1997.
[41] G.M. Sheldrick, SHELXS-97, Program for Refinement of Crystal Structures, University of Göttingen, Germany, 1997.